nature astronomy

SUPPLEMENTARY INFORMATION

https://doi.org/10.1038/s41550-019-0878-9

In the format provided by the authors and unedited.

Water vapour in the atmosphere of the habitable-zone eight-Earth-mass planet K2-18 b

Angelos Tsiaras *, Ingo P. Waldmann *, Giovanna Tinetti , Jonathan Tennyson and Sergey N. Yurchenko

Department of Physics & Astronomy, University College London, London, UK. *e-mail: atsiaras@star.ucl.ac.uk; ingo@star.ucl.ac.uk

Water vapour in the atmosphere of the habitable-zone eight Earth-mass planet K2-18 b

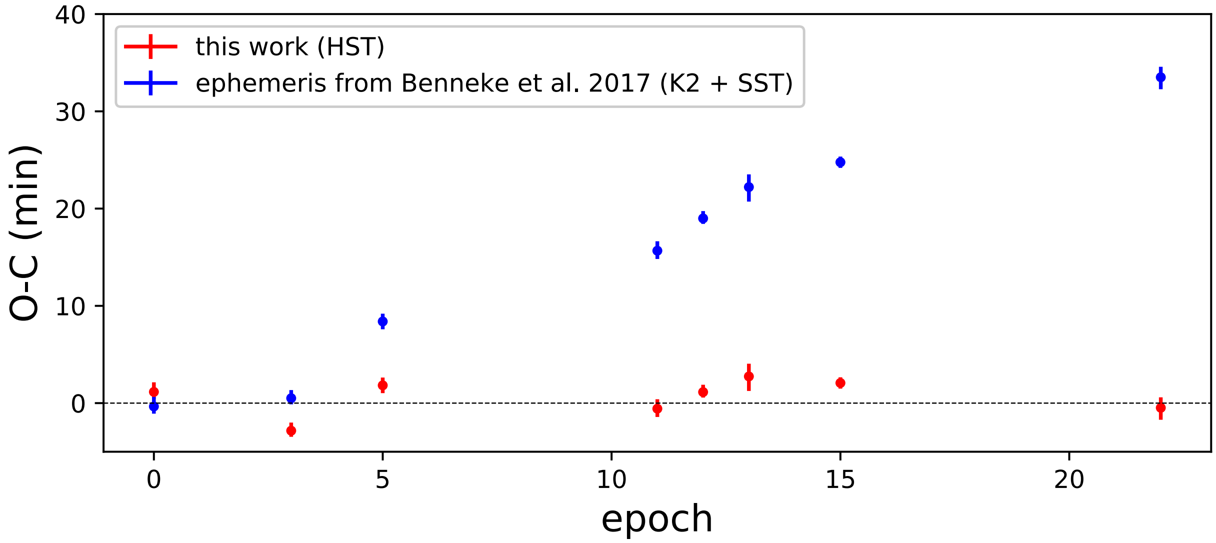

Supplementary Figure 1: O-C diagram using the ephemeris from Benneke et al. 2017 in blue ($P = 32.939622^{0.000099}_{0.000094}$ days and $T_0 = 2457264.39135^{0.00062}_{0.00066}$ $\mathrm{BJD_{UTC}}$) and our updated ephemeris based on the HST data in red ($P = 32.94007 \pm 0.00003$ days and $T_0 = 2457363.2109 \pm 0.0004$ $\mathrm{BJD_{TDB}}$).

Supplementary Table 1: Limb-darkening coefficients for the different wavelength channels.

λ_1 μm	λ_2 μm	a_1	a_2	a_3	a_4
1.1390	1.1730	1.7770	−2.3809	1.9836	−0.6622
1.1730	1.2040	1.7751	−2.3766	1.9665	−0.6526
1.2040	1.2330	1.8060	−2.5127	2.1320	−0.7193
1.2330	1.2610	1.8025	−2.5249	2.1512	−0.7279
1.2610	1.2890	1.8355	−2.6551	2.3012	−0.7866
1.2890	1.3160	1.8596	−2.7798	2.4530	−0.8480
1.3160	1.3420	1.7152	−2.3020	1.9119	−0.6377
1.3420	1.3690	1.4322	−1.3839	0.8815	−0.2404
1.3690	1.3960	1.3984	−1.2141	0.6422	−0.1360
1.3960	1.4230	1.2459	−0.8054	0.2350	0.0087
1.4230	1.4500	1.1758	−0.5644	−0.0498	0.1203
1.4500	1.4780	1.1154	−0.4431	−0.1382	0.1431
1.4780	1.5060	1.1652	−0.5113	−0.1367	0.1590
1.5060	1.5340	1.2015	−0.5856	−0.0719	0.1388
1.5340	1.5620	1.2075	−0.5973	−0.0613	0.1353
1.5620	1.5910	1.3457	−0.9365	0.2415	0.0362
1.5910	1.6200	1.4800	−1.2998	0.6065	−0.0941
1.0880	1.6800	1.5202	−1.5934	1.0698	−0.3030

Supplementary Table 2: Observationally determined parameters of K2-18 b.

Stellar parameters	
[Fe/H] [dex][19]	0.123 ± 0.157
$T_{\rm eff}$ [K][19]	3457 ± 39
M_* [$M_\odot$][19]	0.359 ± 0.047
R_* [$R_\odot$][19]	0.411 ± 0.038
Planetary parameters	
$T_{\rm eq}$ [K][22] Bond albedo = 0.3	235 ± 9
$M_{\rm p}$ [$M_\oplus$][22]	7.96 ± 1.91
$R_{\rm p}$ [$R_\oplus$][19]	$2.279^{+0.026}_{-0.025}$
a [AU][19]	$0.1429^{+0.0060}_{-0.0065}$
Transit parameters - this study	
T_0 [days, BJD$_{\rm TDB}$]	2457363.2109 ± 0.0004
Period [days]	32.94007 ± 0.00003
$R{\rm p}/R_*$ (WFC3 − G141 band)	0.05405 ± 0.00014
a/R_*	81.3 ± 1.5
i [deg]	89.56 ± 0.02

Supplementary Table 3: Fitting results and residuals diagnostics for the eight different white light curves (R^2: autocorelation, $\overline{\sigma}$: standard deviation relative to photon noise, $\overline{\chi}^2$: reduced χ^2 calculated with the rescaled uncertainties).

T_0 HJD$_{\mathrm{UTC}}$	T_0 BJD$_{\mathrm{TDB}}$	$(R_p/R_*)^2$ ppm	R^2	$\overline{\sigma}$	$\overline{\chi}^2$
$2457363.2101^{+0.0003}_{-0.0002}$	$2457363.210869^{+0.0003}_{-0.0002}$	2928^{+39}_{-39}	0.07	1.84	1.14
$2457462.02922^{+0.00023}_{-0.00017}$	$2457462.029990^{+0.00023}_{-0.00017}$	2873^{+38}_{-33}	0.11	2.1	1.14
$2457527.9107^{+0.0002}_{-0.0002}$	$2457527.911470^{+0.0002}_{-0.0002}$	2944^{+49}_{-43}	0.17	2.04	1.14
$2457725.5504^{+0.0003}_{-0.0002}$	$2457725.551173^{+0.0003}_{-0.0002}$	2931^{+33}_{-25}	0.21	1.78	1.16
$2457758.49096^{+0.00021}_{-0.00016}$	$2457758.49096^{+0.00021}_{-0.00016}$	2968^{+51}_{-45}	0.27	2.1	1.15
$2457791.4315^{+0.0004}_{-0.0004}$	$2457791.432286^{+0.0004}_{-0.0004}$	2921^{+54}_{-47}	0.24	2.39	1.19
$2457857.31143^{+0.00016}_{-0.00016}$	$2457857.312218^{+0.00016}_{-0.00016}$	2918^{+41}_{-36}	0.15	1.84	1.13
$2458087.8912^{+0.0003}_{-0.0003}$	$2458087.891996^{+0.0003}_{-0.0003}$	2888^{+83}_{-55}	0.16	2.55	1.22

Supplementary Table 4: Fitting results and residuals diagnostics for the different wavelength channels (R^2: autocorrelation, $\overline{\sigma}$: standard deviation relative to photon noise, $\overline{\chi}^2$: reduced χ^2). The diagnostics are presented as the mean and the standard deviation of the eight visits. Information on individual visits can be found in Supplementary Figures 3 to 19.

λ_1 μm	λ_2 μm	$(R_\mathrm{p}/R_*)^2$ ppm	R^2 $\mu\,(\sigma)$	$\overline{\sigma}$ $\mu\,(\sigma)$	$\overline{\chi}^2$ $\mu\,(\sigma)$
1.1390	1.1730	2905 ± 25	0.13 (0.08)	1.09 (0.08)	1.060 (0.007)
1.1730	1.2040	2939 ± 26	0.13 (0.04)	1.12 (0.10)	1.060 (0.006)
1.2040	1.2330	2903 ± 24	0.13 (0.05)	1.07 (0.05)	1.061 (0.007)
1.2330	1.2610	2922 ± 25	0.15 (0.06)	1.08 (0.10)	1.061 (0.007)
1.2610	1.2890	2891 ± 26	0.14 (0.08)	1.16 (0.17)	1.059 (0.008)
1.2890	1.3160	2918 ± 26	0.11 (0.06)	1.13 (0.16)	1.061 (0.006)
1.3160	1.3420	2919 ± 24	0.15 (0.07)	1.09 (0.13)	1.061 (0.007)
1.3420	1.3690	2965 ± 24	0.13 (0.05)	1.05 (0.08)	1.061 (0.007)
1.3690	1.3960	2955 ± 27	0.15 (0.09)	1.17 (0.07)	1.062 (0.007)
1.3960	1.4230	2976 ± 25	0.16 (0.06)	1.10 (0.08)	1.061 (0.006)
1.4230	1.4500	2990 ± 24	0.12 (0.09)	1.01 (0.08)	1.061 (0.007)
1.4500	1.4780	2895 ± 23	0.18 (0.06)	1.02 (0.09)	1.061 (0.006)
1.4780	1.5060	2930 ± 23	0.15 (0.07)	1.04 (0.08)	1.061 (0.007)
1.5060	1.5340	2921 ± 24	0.12 (0.06)	1.05 (0.08)	1.062 (0.006)
1.5340	1.5620	2875 ± 24	0.15 (0.07)	1.02 (0.06)	1.061 (0.006)
1.5620	1.5910	2927 ± 25	0.13 (0.09)	1.10 (0.08)	1.061 (0.006)
1.5910	1.6200	2925 ± 24	0.13 (0.06)	1.14 (0.16)	1.063 (0.009)

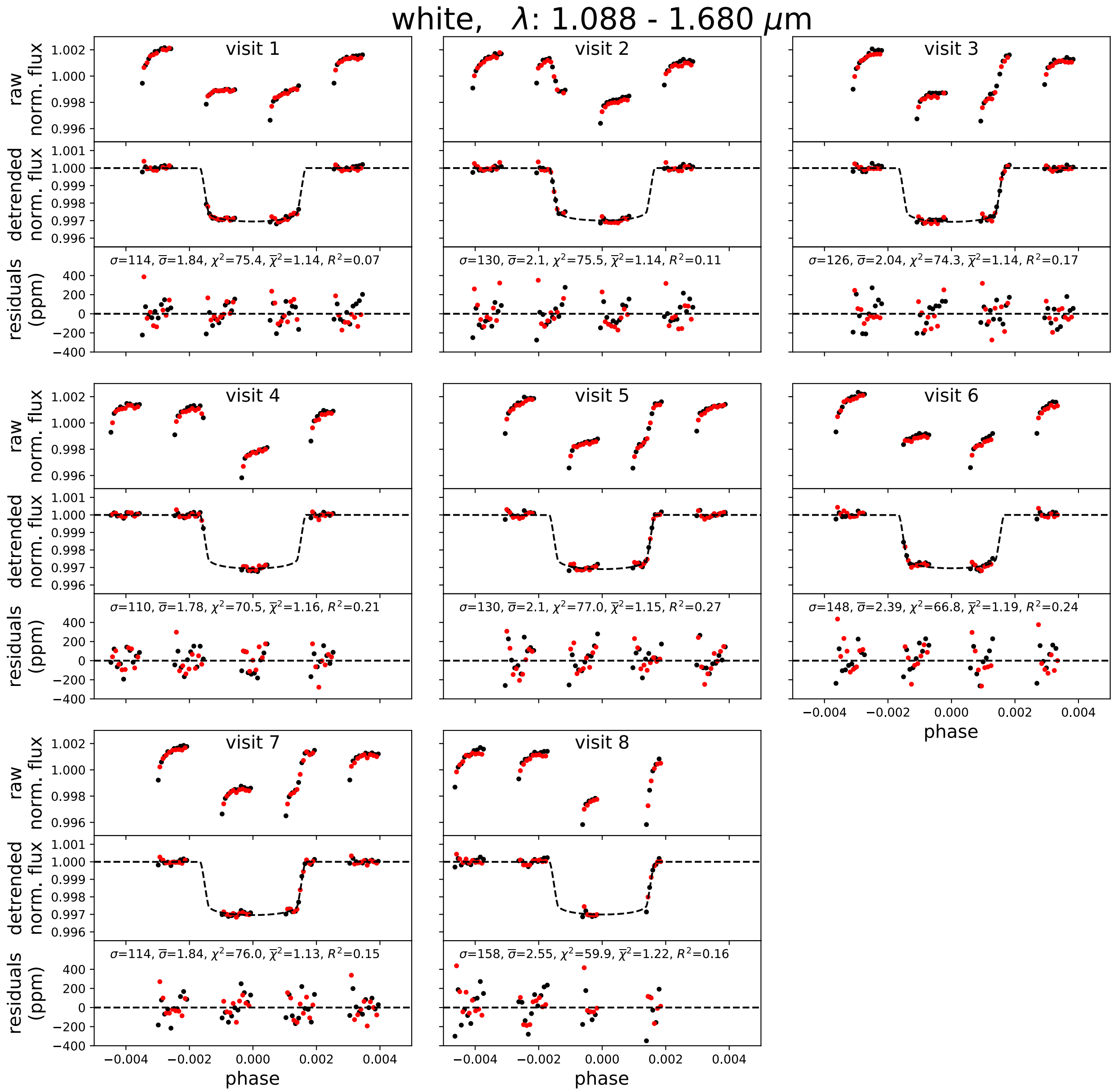

Supplementary Figure 2: Analysis of the eight K2-18 b white light curves, for the forward (black) and reverse (red) scans. In each subplot, from top to bottom: A) Raw light curves extracted from the HST observations. B) Raw light curves divided by the best-fit model for the systematics. C) Fitting residuals where their standard deviation (σ), their standard deviation relatively to the photon noise ($\overline{\sigma}$), their chi squared (χ^2), their reduced chi squared ($\overline{\chi}^2$), and their autocorrelation (R^2).

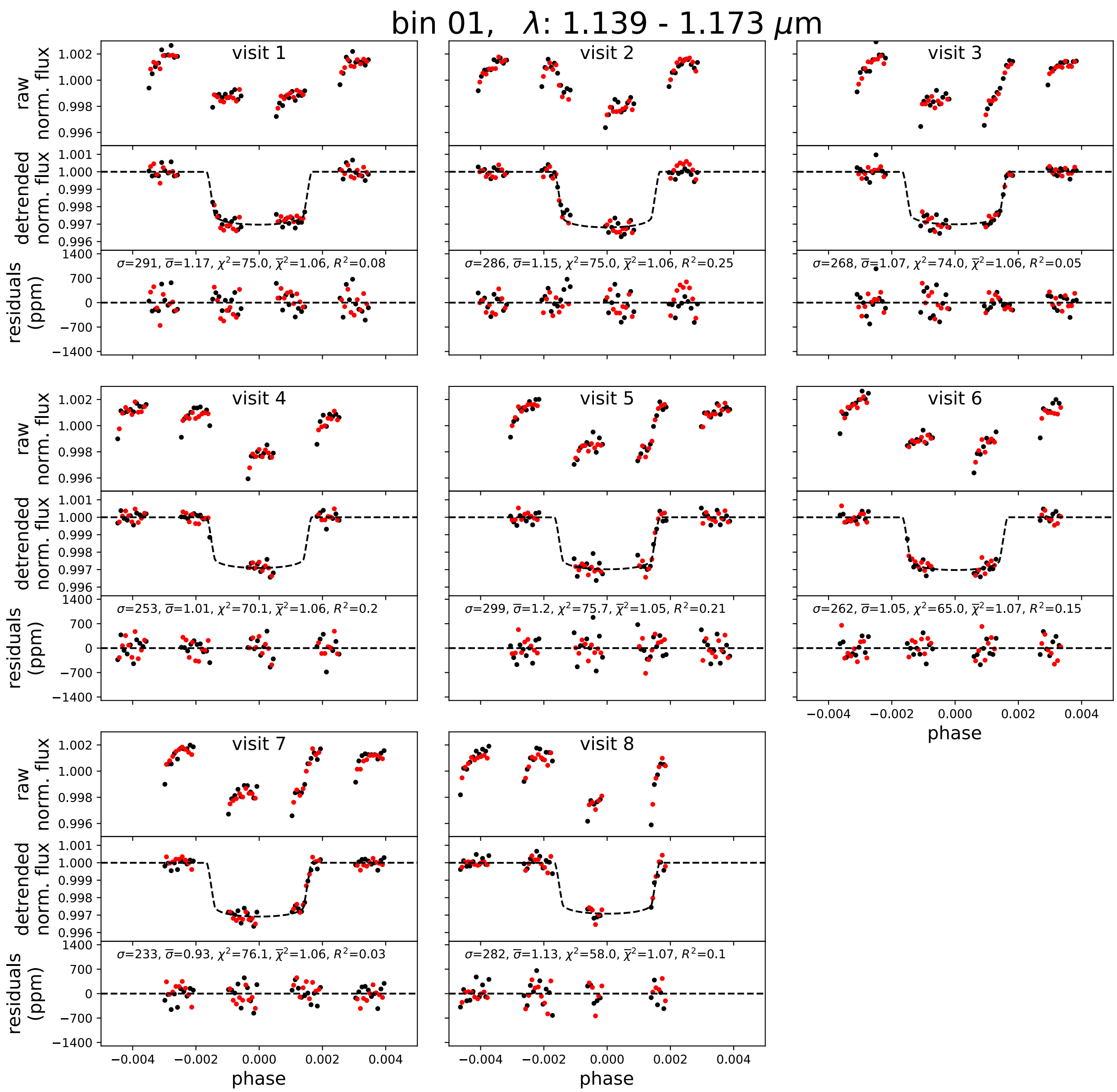

Supplementary Figure 3: Same as Supplementary Figure 2 for the spectral channel between 1.139 and 1.173 μm.

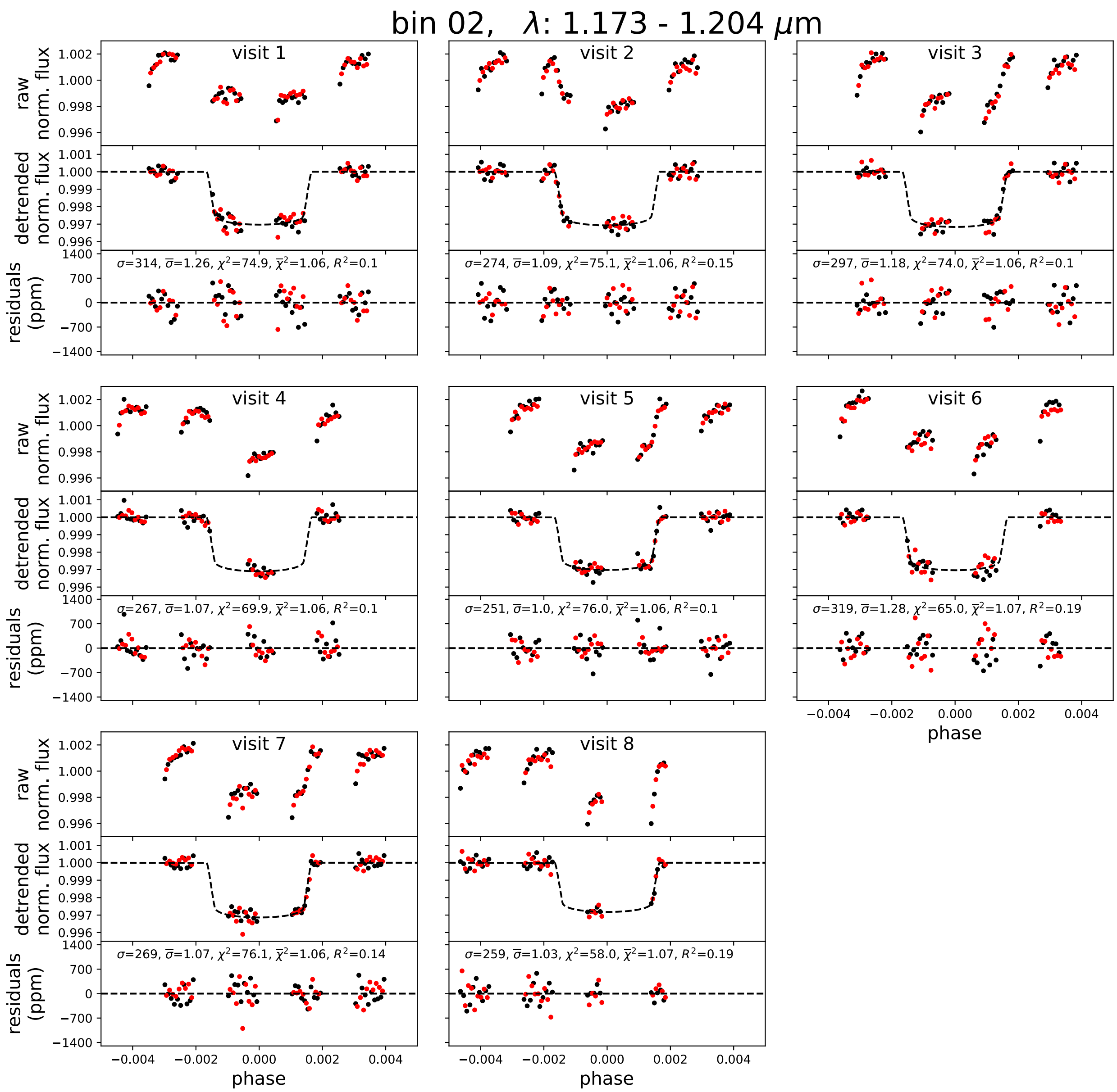

Supplementary Figure 4: Same as Supplementary Figure 2 for the spectral channel between 1.173 and 1.204 μm.

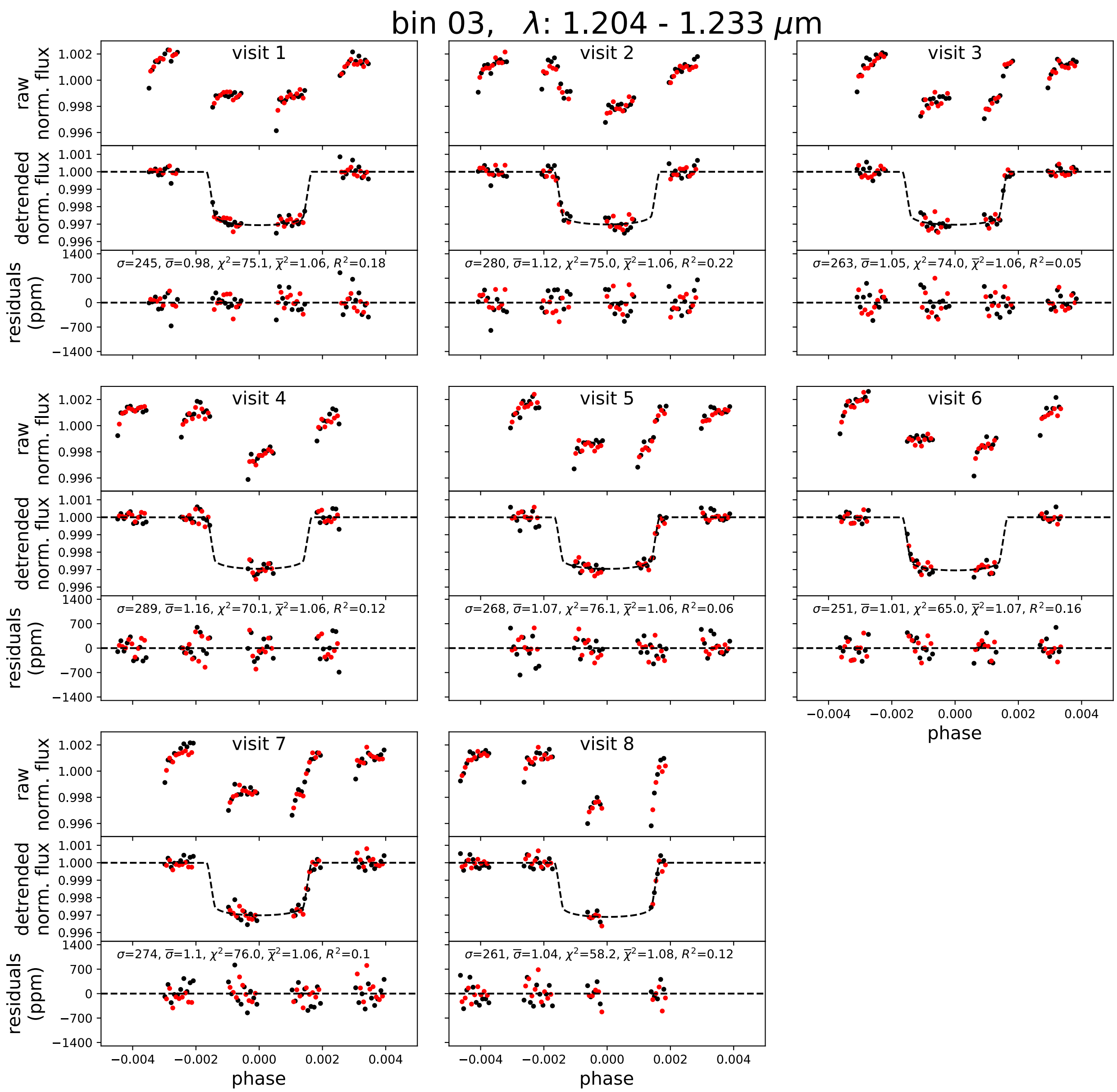

Supplementary Figure 5: Same as Supplementary Figure 2 for the spectral channel between 1.204 and 1.233 μm.

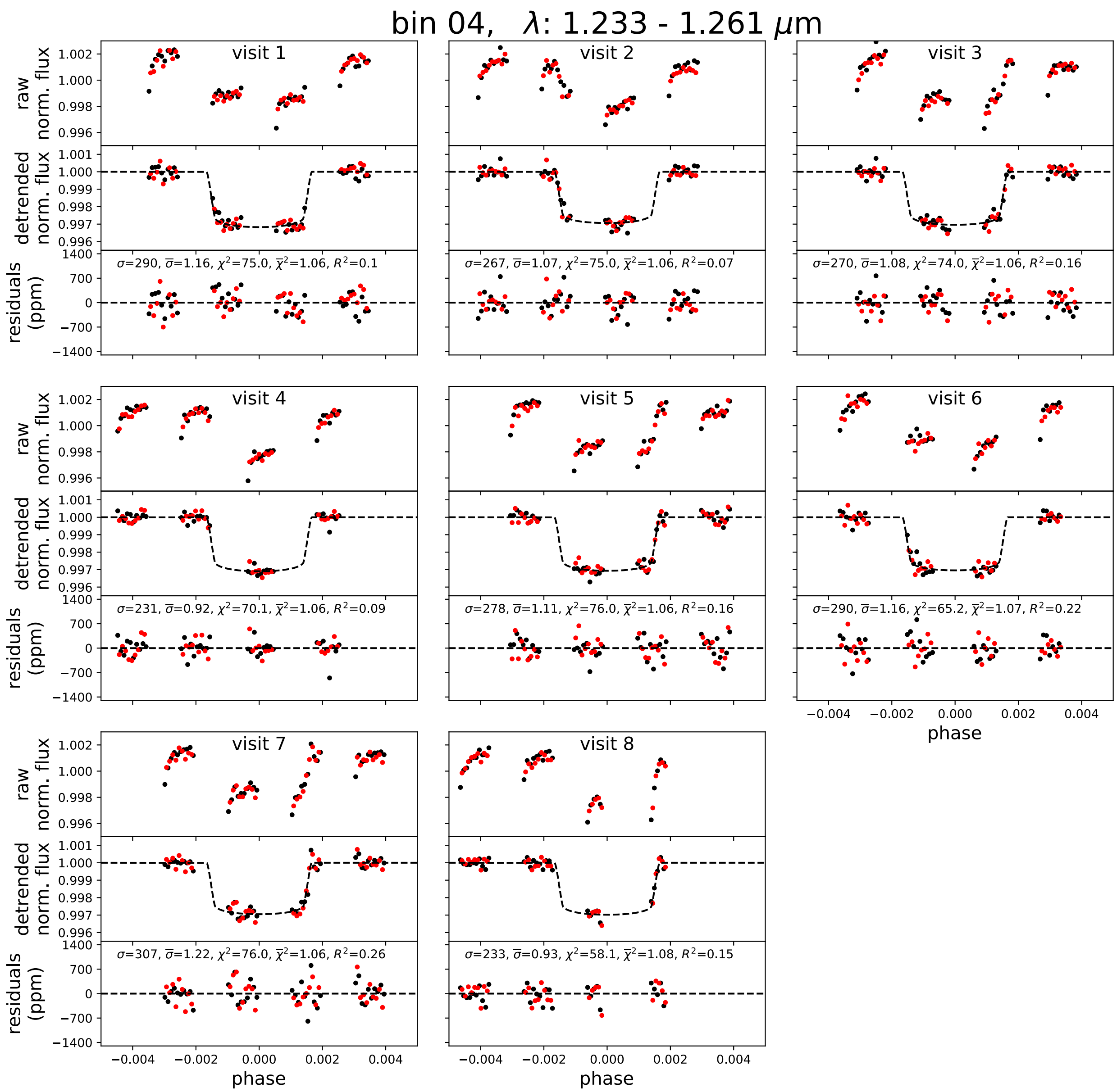

Supplementary Figure 6: Same as Supplementary Figure 2 for the spectral channel between 1.233 and 1.261 μm.

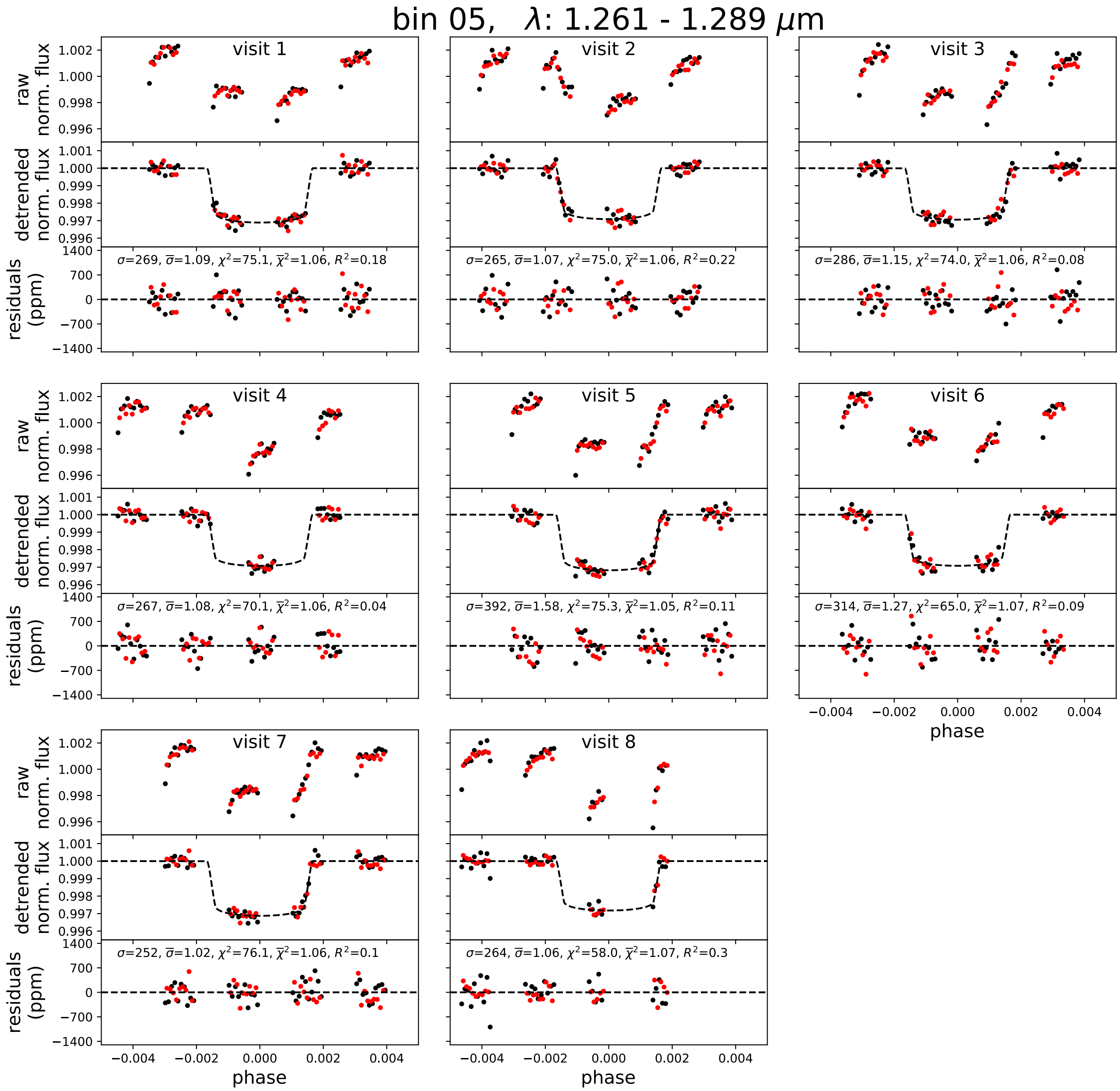

Supplementary Figure 7: Same as Supplementary Figure 2 for the spectral channel between 1.261 and 1.289 μm.

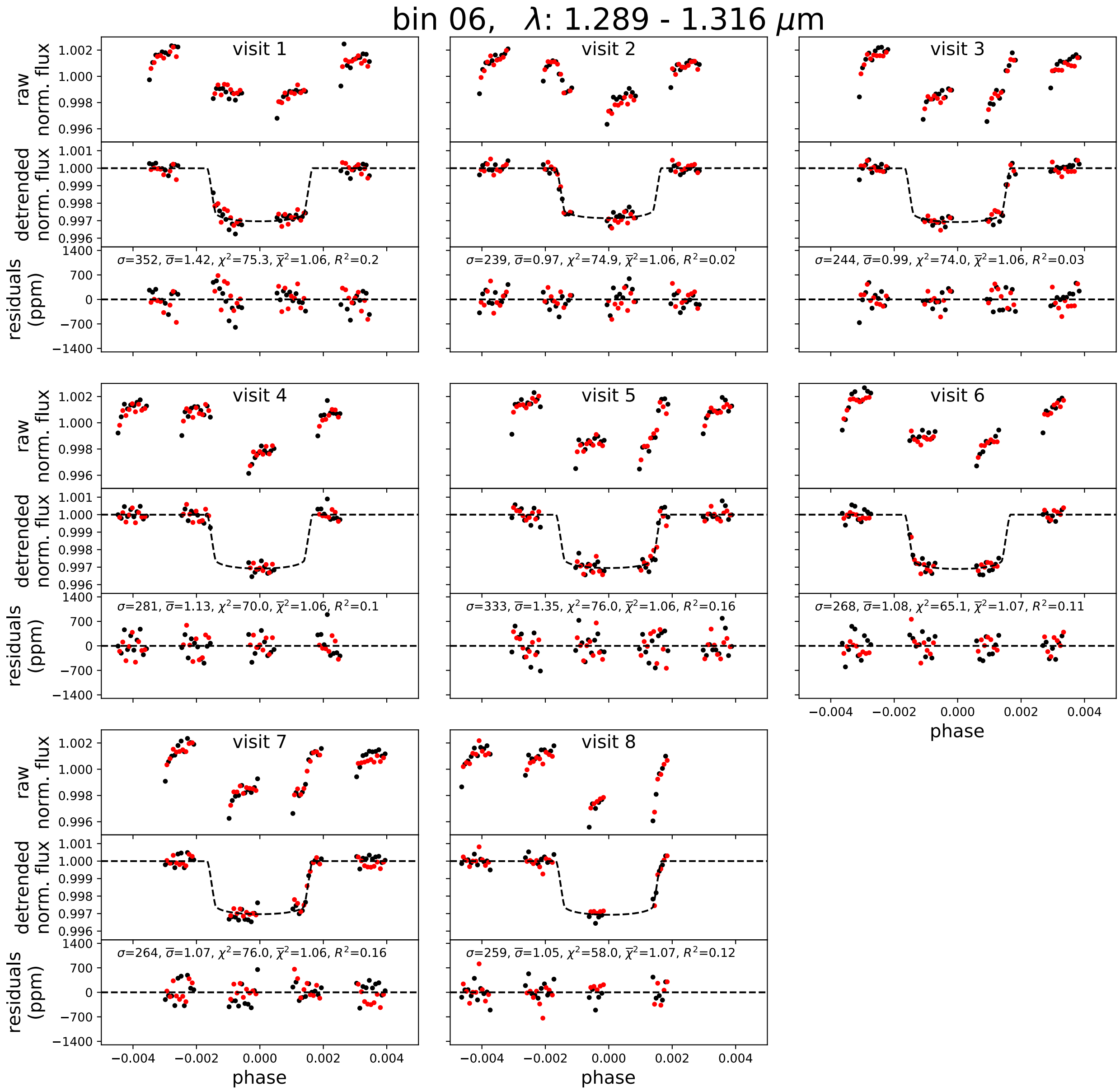

Supplementary Figure 8: Same as Supplementary Figure 2 for the spectral channel between 1.289 and 1.316 μm.

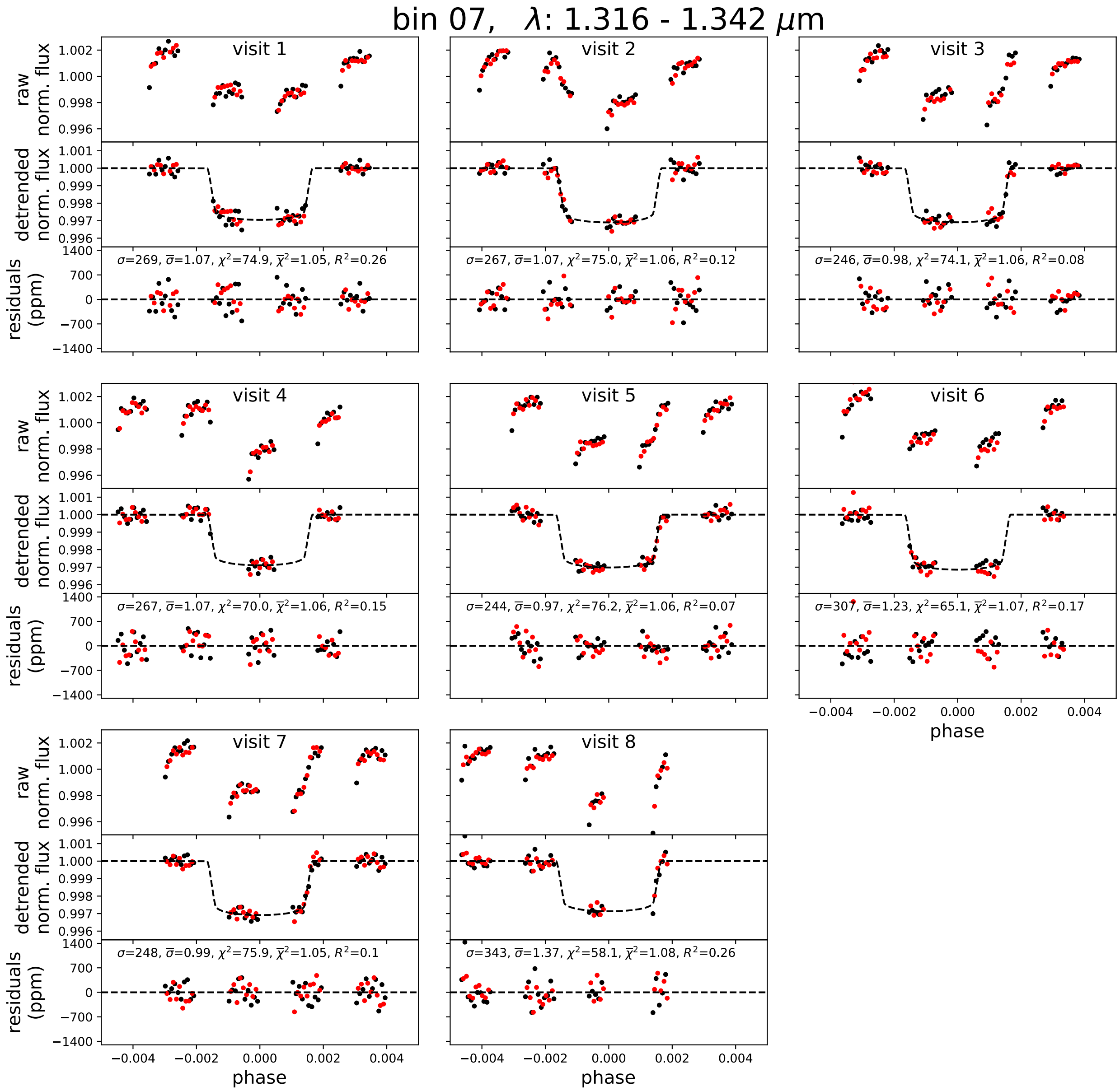

Supplementary Figure 9: Same as Supplementary Figure 2 for the spectral channel between 1.316 and 1.342 μm.

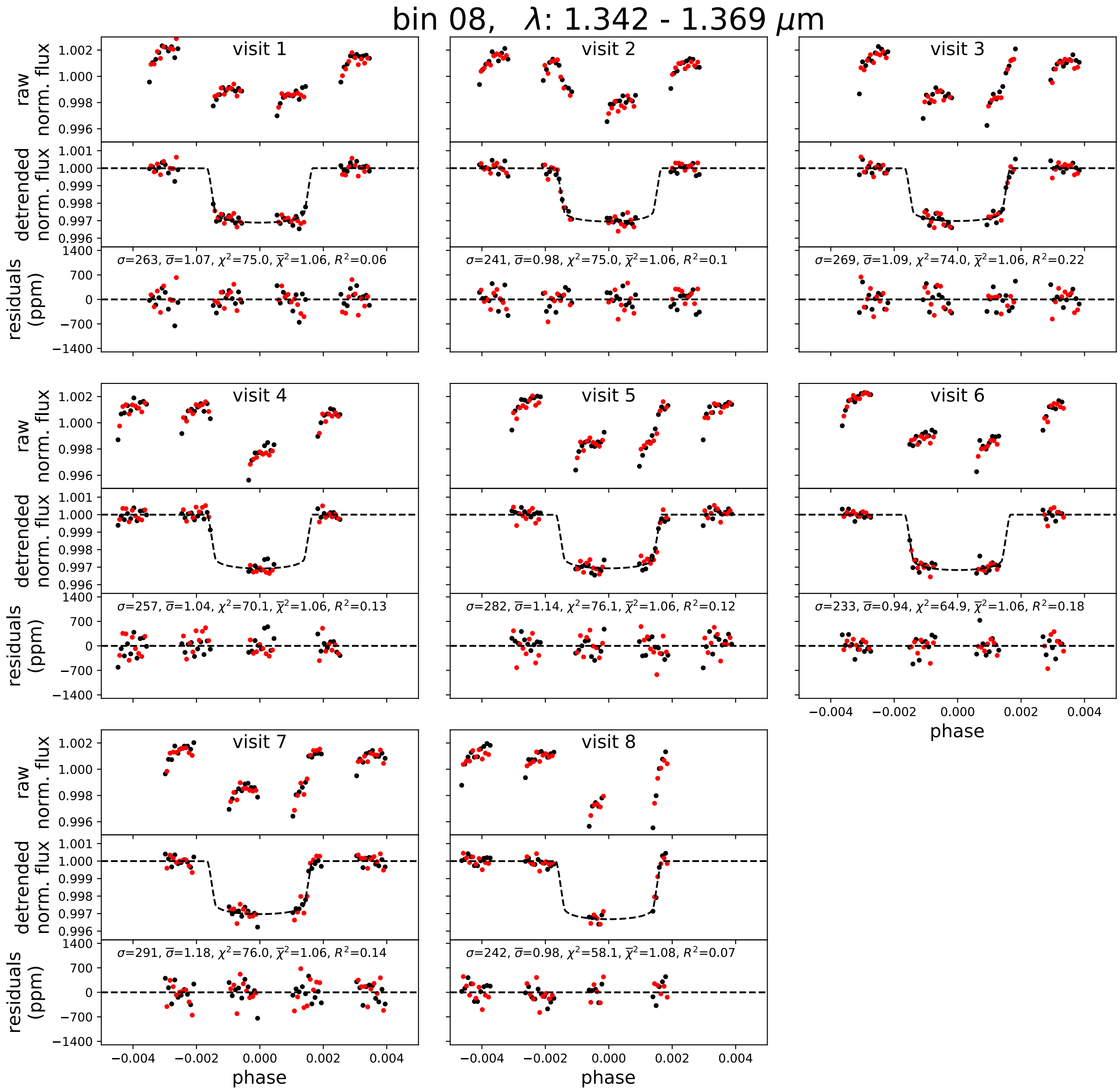

Supplementary Figure 10: Same as Supplementary Figure 2 for the spectral channel between 1.342 and 1.369 μm.

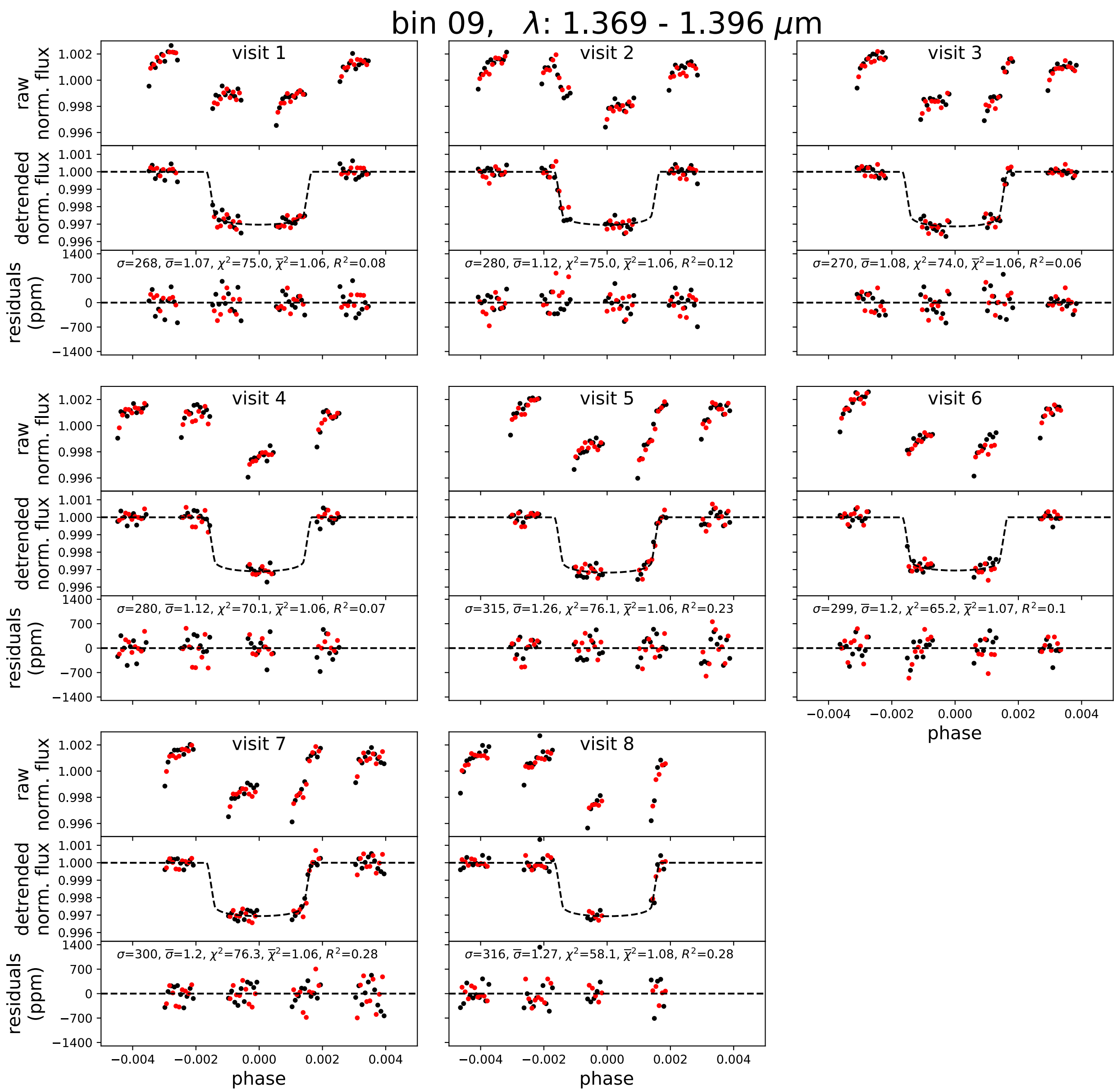

Supplementary Figure 11: Same as Supplementary Figure 2 for the spectral channel between 1.369 and 1.396 μm.

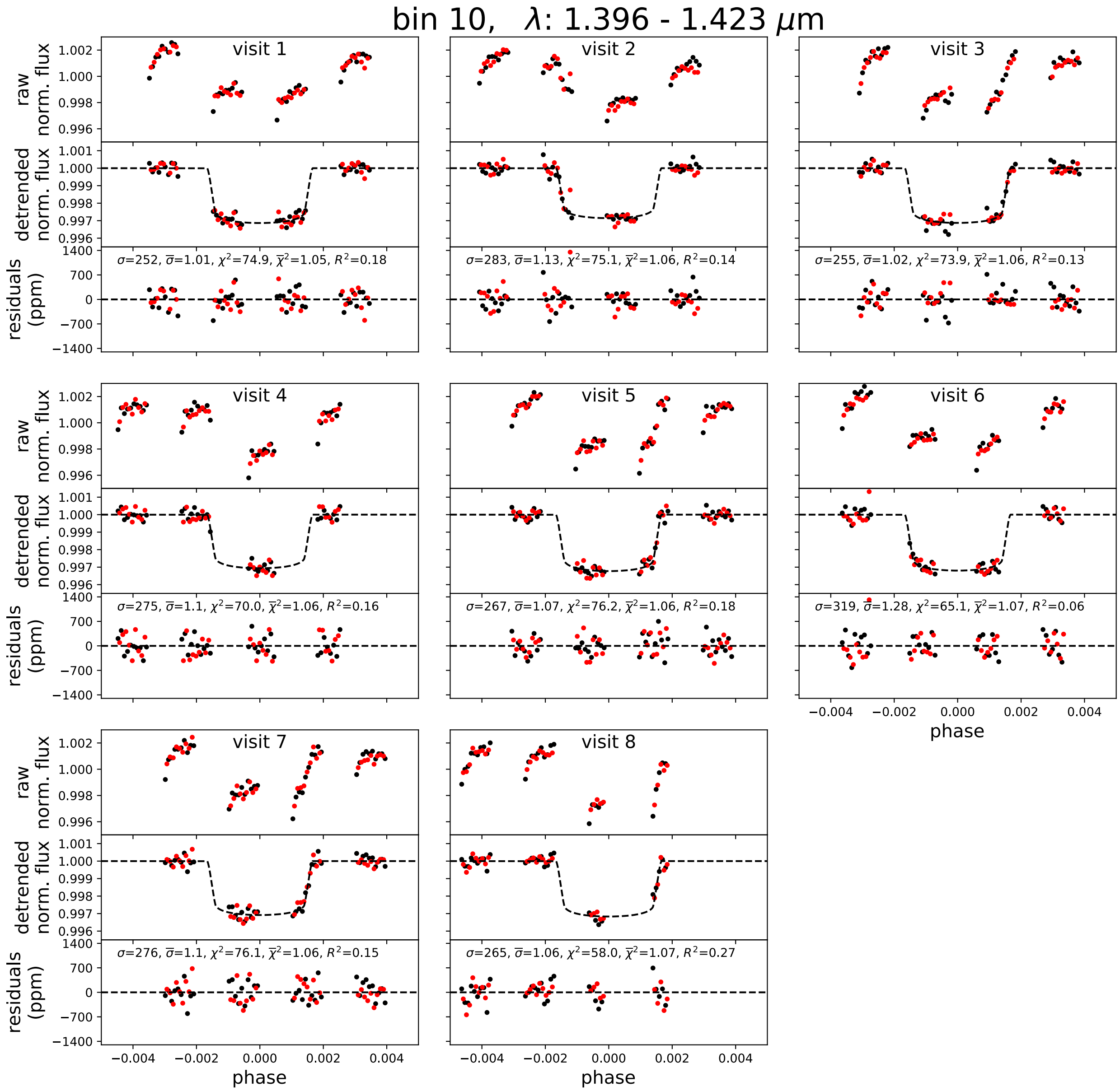

Supplementary Figure 12: Same as Supplementary Figure 2 for the spectral channel between 1.396 and 1.423 μm.

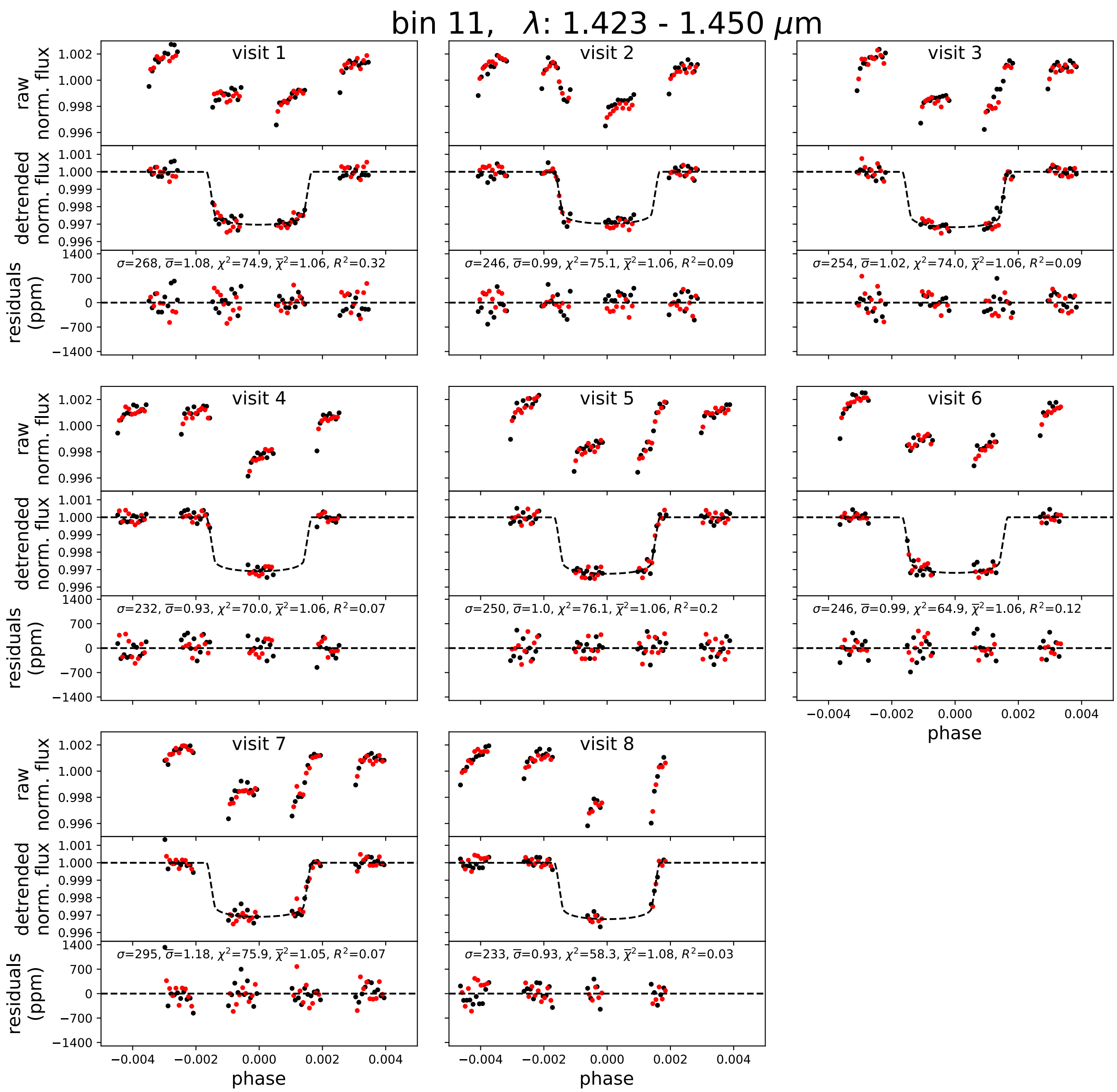

Supplementary Figure 13: Same as Supplementary Figure 2 for the spectral channel between 1.423 and 1.450 μm.

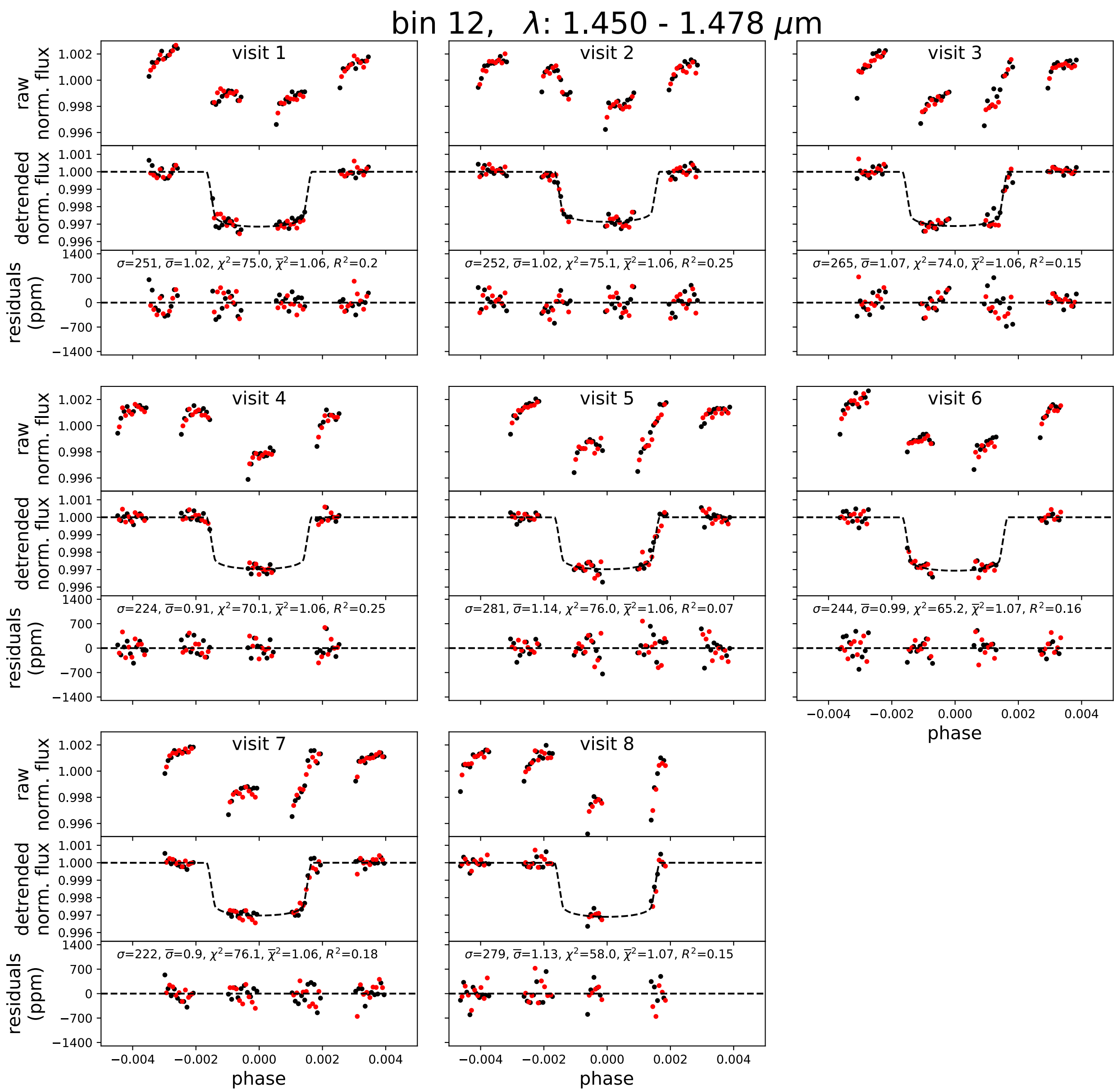

Supplementary Figure 14: Same as Supplementary Figure 2 for the spectral channel between 1.450 and 1.478 μm.

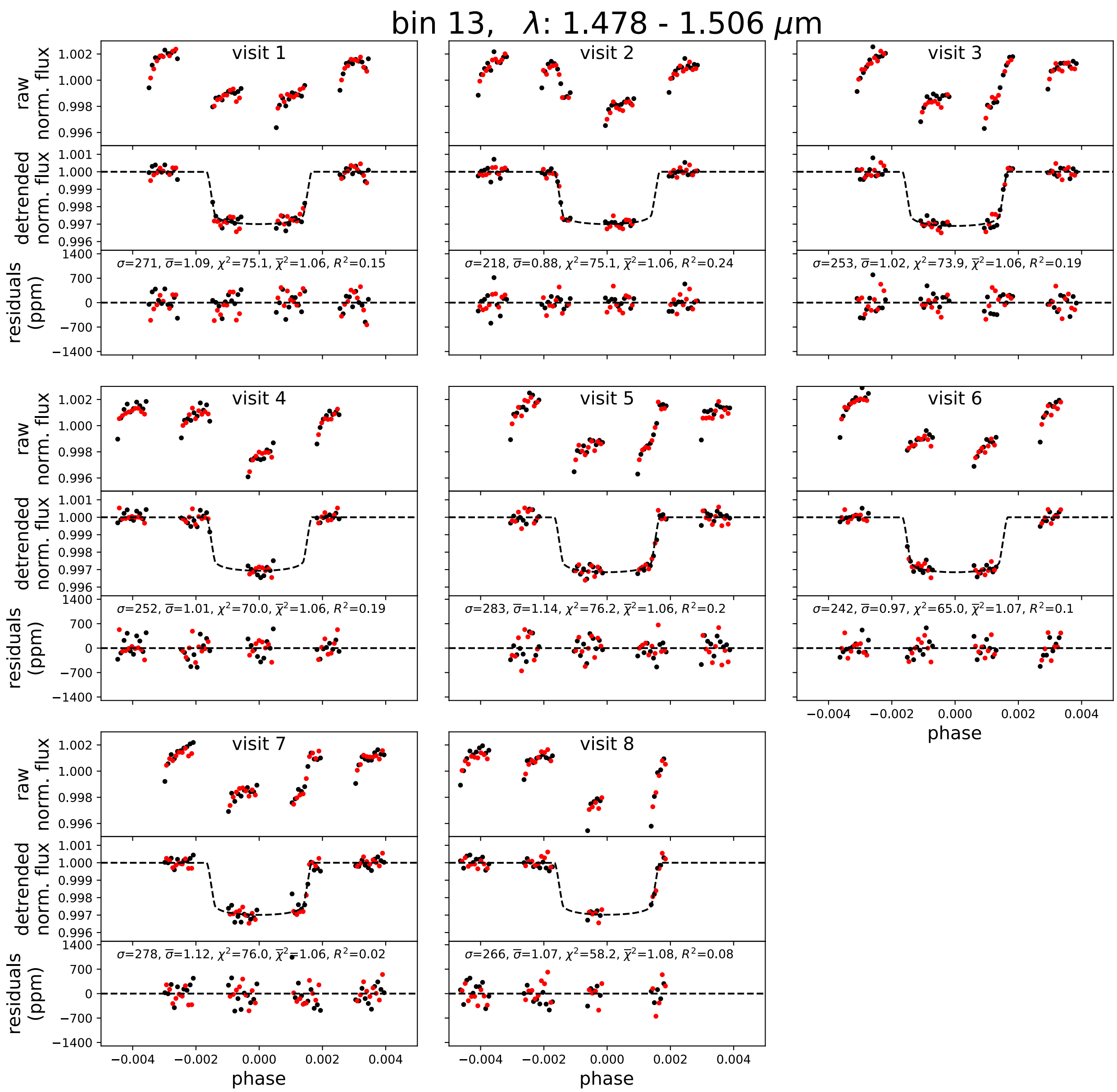

Supplementary Figure 15: Same as Supplementary Figure 2 for the spectral channel between 1.478 and 1.506 μm.

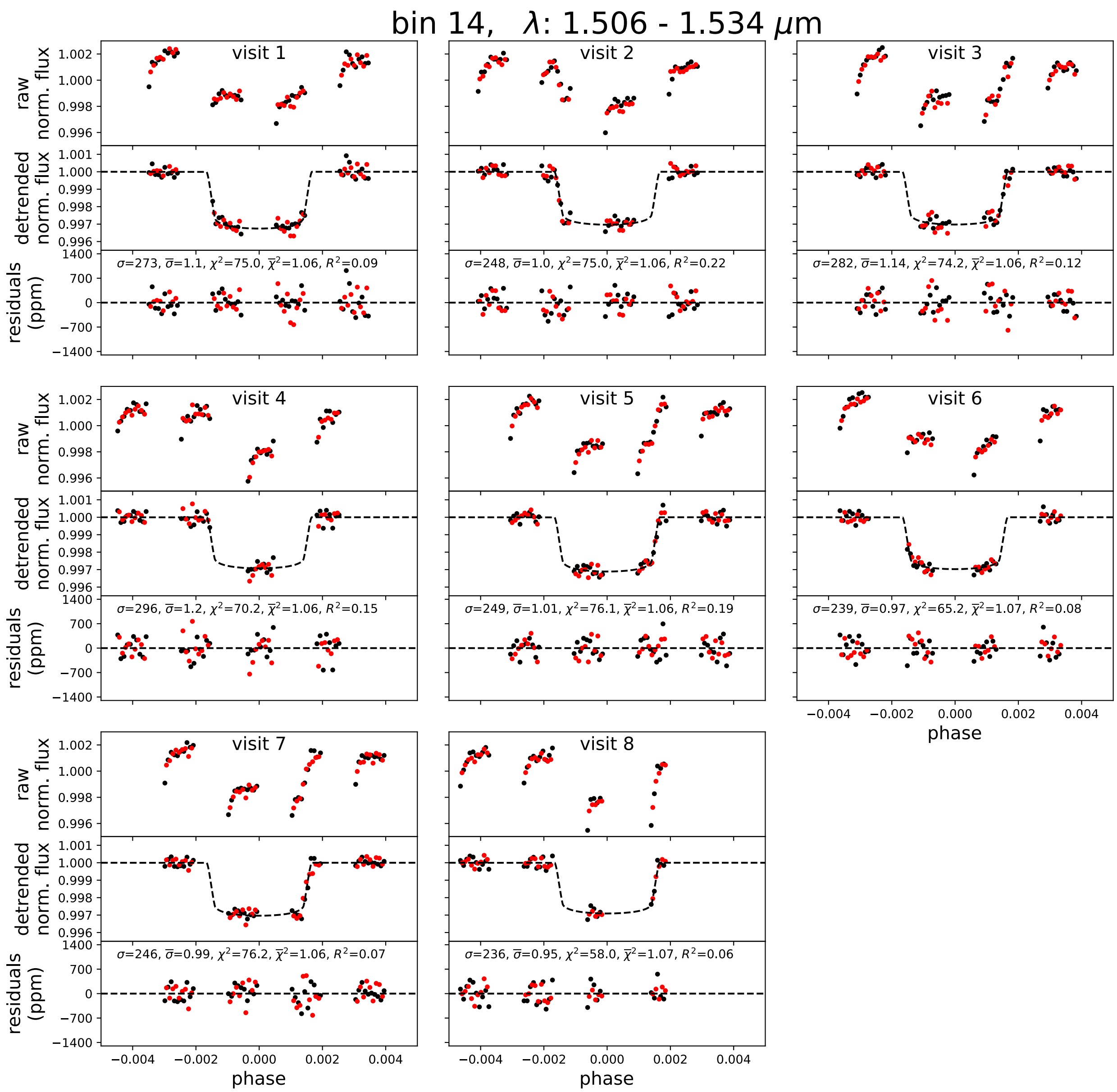

Supplementary Figure 16: Same as Supplementary Figure 2 for the spectral channel between 1.506 and 1.534 μm.

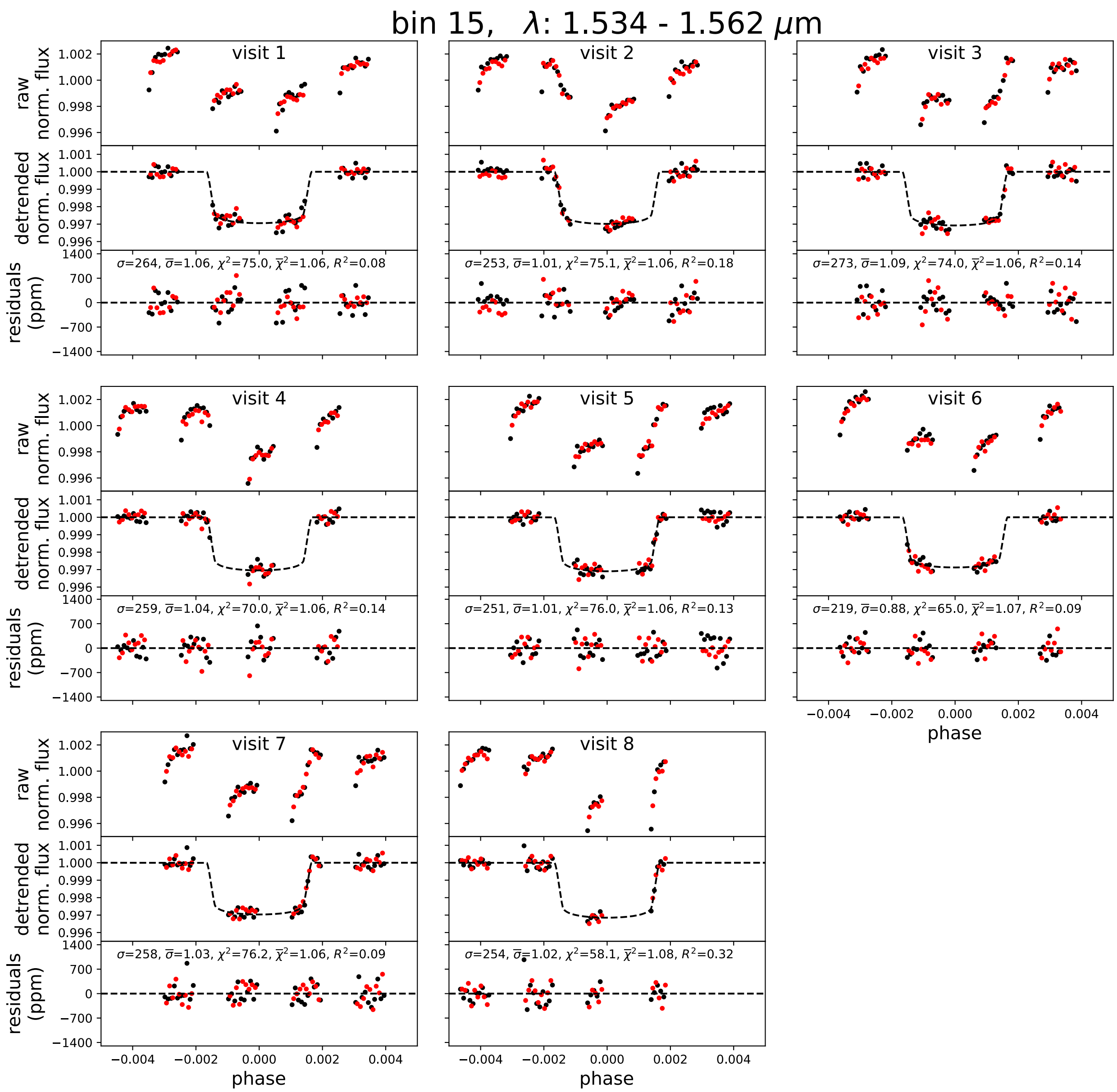

Supplementary Figure 17: Same as Supplementary Figure 2 for the spectral channel between 1.534 and 1.562 μm.

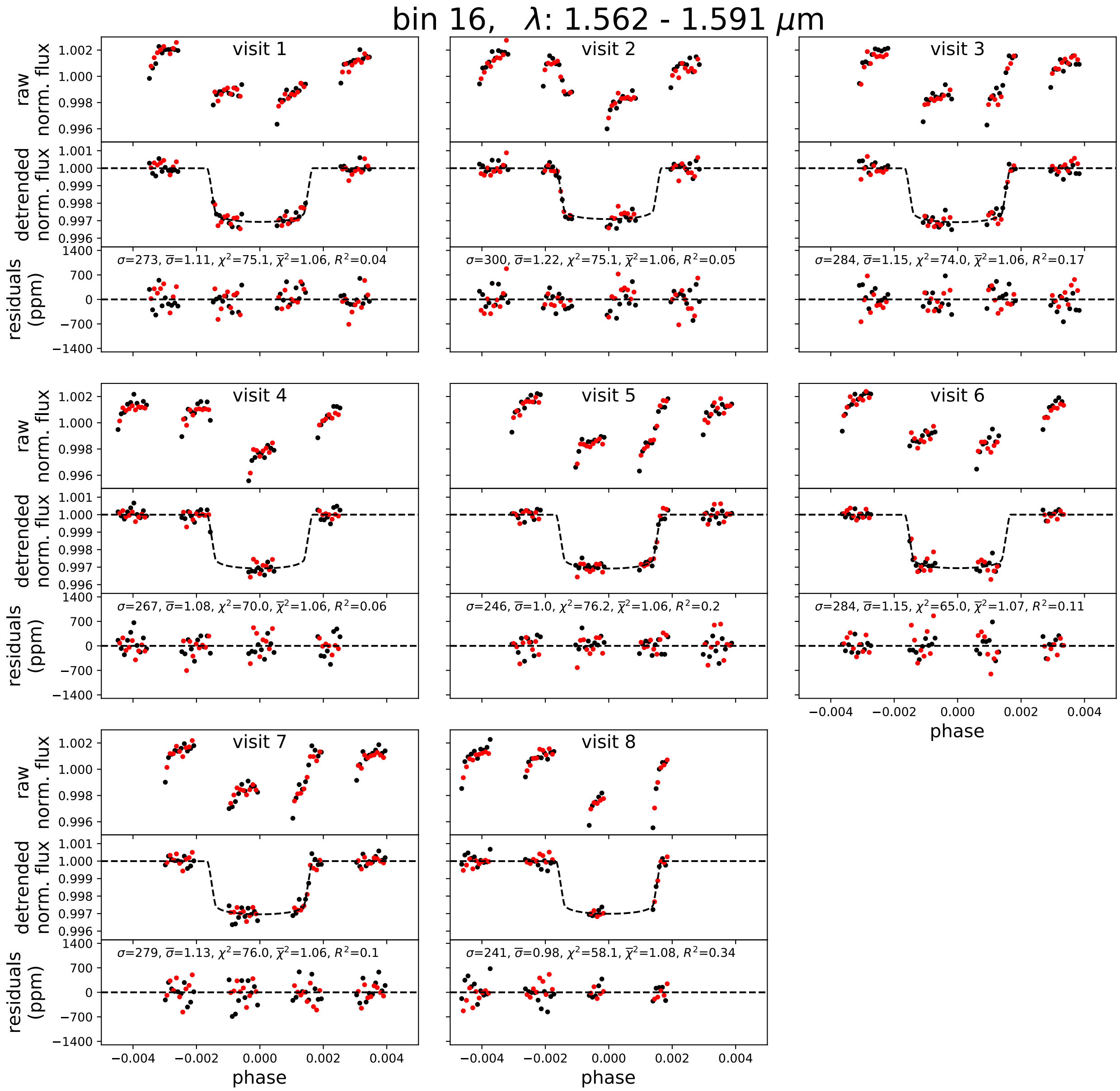

Supplementary Figure 18: Same as Supplementary Figure 2 for the spectral channel between 1.562 and 1.591 μm.

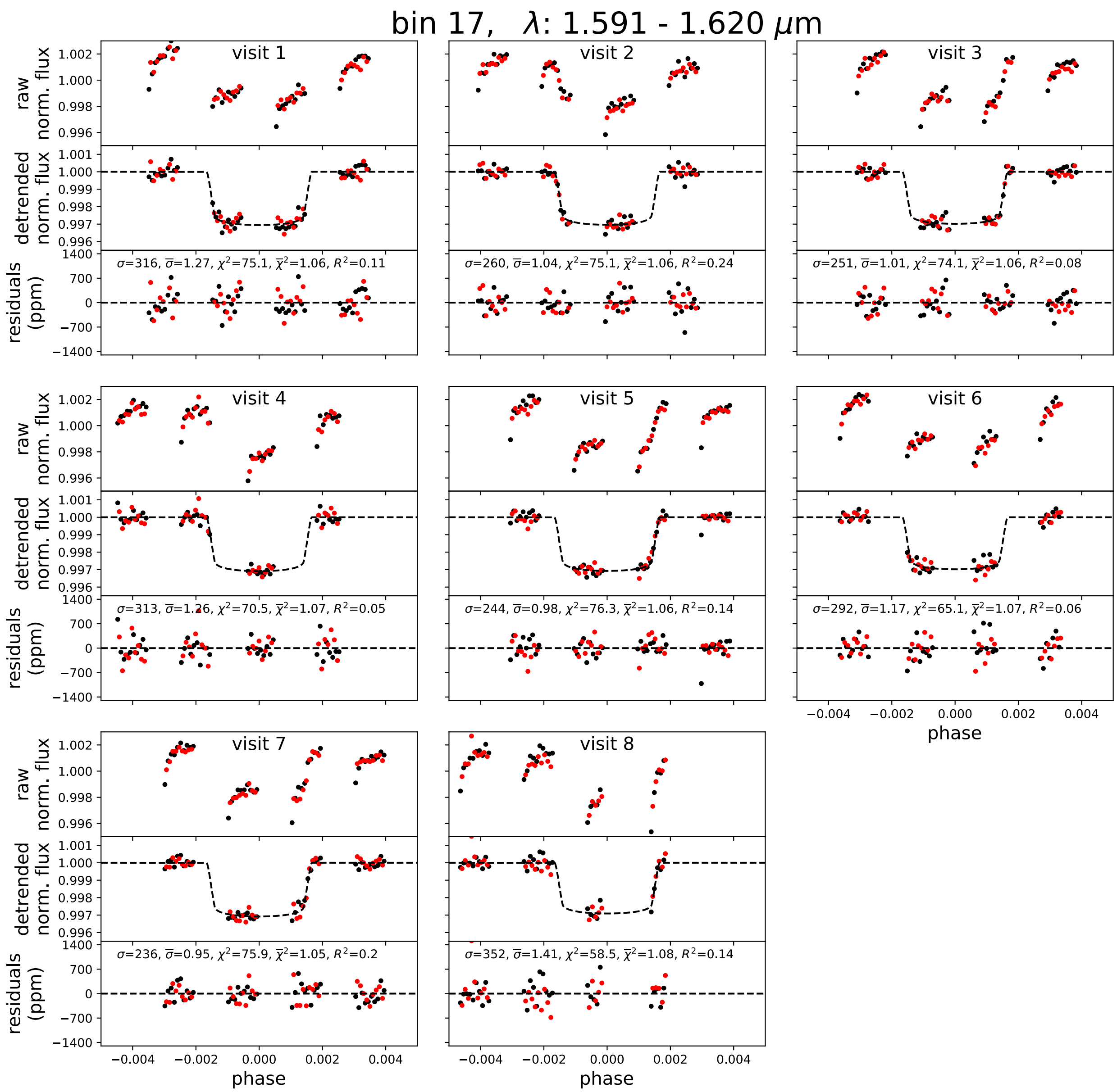

Supplementary Figure 19: Same as Supplementary Figure 2 for the spectral channel between 1.591 and 1.620 μm.

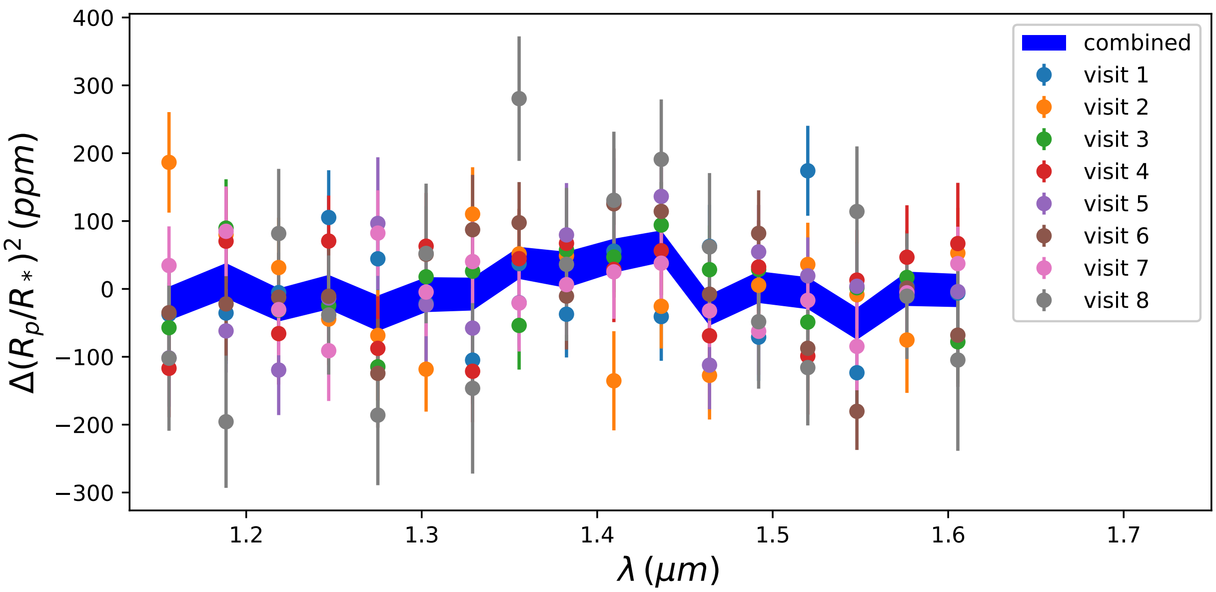

Supplementary Figure 20: Mean-subtracted spectra extracted per visits, and the final, reported, weighted average.

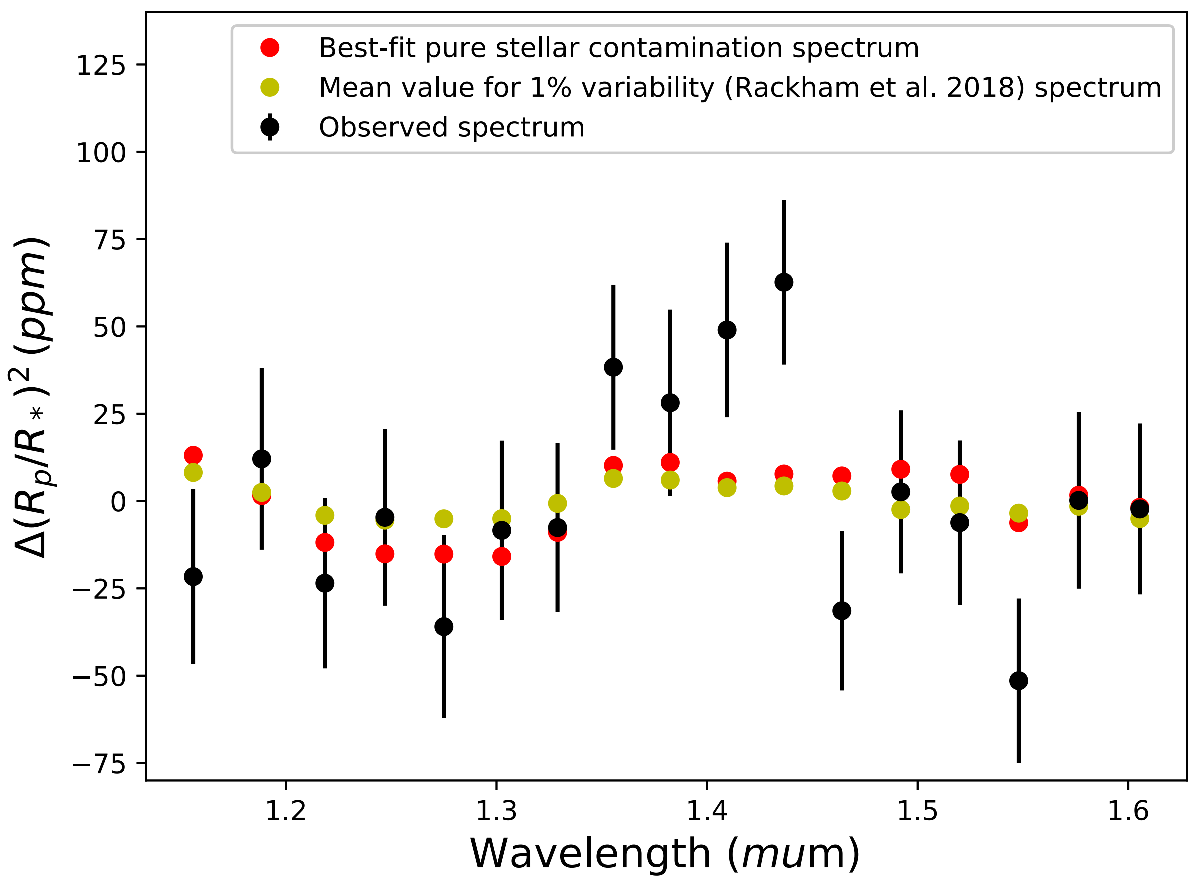

Supplementary Figure 21: Comparison between the observed spectrum and spectra produced only by the effect of spots and faculae (assuming no contribution from the planet). The yellow spectrum corresponds to the mean spot and faculae coverage predicted by Rackham et al. 2018[41] for an M2 star and 1% I-band variability (19%, 72%, respectively). The red spectrum corresponds to the best-fit contamination model to the observed spectrum (26%, 73%, respectively). From this, we conclude that pure stellar contamination cannot explain the observed water feature.